Redox Biology 14 (2018) 237–249

Contents lists available at ScienceDirect

Redox Biology

journal homepage: www.elsevier.com/locate/redox

Butaselen prevents hepatocarcinogenesis and progression through inhibiting thioredoxin reductase activity

Xiaoqing Zheng[a,b,1], Weiwei Ma[a,b,1], Ruoxuan Sun[a,b], Hanwei Yin[c], Fei Lin[d], Yuxi Liu[a,b], Wei Xu[e], Huihui Zeng[a,b,*]

[a] State Key Laboratory of Natural and Biomimetic Drugs, No. 38, Xueyuan Road, Beijing 100191, PR China
[b] Department of Chemical Biology, School of Pharmaceutical Sciences, Peking University, No. 38, Xueyuan Road, Beijing 100191, PR China
[c] Keaise Center for Clinical Laboratory, No. 666, Gaoxin Road, Wuhan 430000, PR China
[d] National Institutes for Food and Drug Control, No. 2, Tiantanxili, Beijing 100050, PR China
[e] Department of Pharmacology and Molecular Sciences, Johns Hopkins University School of Medicine, Baltimore, MD 21287, USA

ARTICLE INFO

Keywords:
Chemoprevention
Hepatocellular carcinoma (HCC)
Thioredoxin reductase (TrxR)
NF-κB
Reactive oxygen species (ROS)

ABSTRACT

Hepatocellular carcinoma (HCC) accounts for most of primary liver cancer, of which five-year survival rate remains low and chemoprevention has become a strategy to reduce disease burden of HCC. We aim to explore the *in vivo* chemopreventive effect of an organoselenium-containing compound butaselen (BS) against hepatocarcinogenesis and its underlying mechanisms. Pre- and sustained BS treatment (9, 18 and 36 mg/Kg BS) could dose-dependently inhibit chronic hepatic inflammation, fibrosis, cirrhosis and HCC on murine models with 24 weeks treatment scheme. The thioredoxin reductase (TrxR), NF-κB pathway and pro-inflammatory factors were activated during hepatocarcinogenesis, while their expression were decreased by BS treatment. BS treatment could also significantly reduce tumor volume in H22-bearing models and remarkably slow tumor growth. HCC cell lines HepG2, Bel7402 and Huh7 were time- and dose-dependently inhibited by BS treatment. G2/M arrest and apoptosis were observed in HepG2 cells after BS treatment, which were mediated by TrxR/Ref-1 and NF-κB pathways inhibition. BS generated reactive oxygen species (ROS), which could be reduced by antioxidant N-acetyl-L-cysteine (NAC) and NADPH oxidase inhibitor DPI. NAC could markedly increase HepG2 cells viability. TrxR activity of HepG2 cells treated with BS were significantly decreased in parallel with proliferative inhibition. The TrxR1-knockdown HepG2 cells also exhibited low TrxR1 activity, high ROS level, relatively low proliferation rate and increased resistance to BS treatment. In conclusion, BS can prevent hepatocarcinogenesis through inhibiting chronic inflammation, cirrhosis and tumor progression. The underlying mechanisms may include TrxR activity inhibition, leading to ROS elevation, G2/M arrest and apoptosis.

1. Introduction

Primary liver cancer ranks the sixth most common cancer worldwide; what is worse, it ranks as the second most common causes of cancer death around the world [1]. 70–90% primary liver cancer is classified as hepatocellular carcinoma (HCC). Major high-risk factors for HCC include virus infection (HBV, HCV), aflatoxin B1 and alcohol abuse. Hepatocarcinogenesis is closely correlated with cirrhosis, which develops after 20–40 years of chronic liver inflammation and will increase the risk of HCC exponentially. [2]. Current therapeutic regimes includes resection, ablation and transplantation for early stage HCC; chemoembolization and sorafenib for intermediate and advanced stage HCC respectively [3]. However, most patients cannot be diagnosed at early stage, resulting in delayed treatment; besides, recurrence is of high frequency due to microscopic dissemination [4], which ultimately lead to only 20–40% five-year survival rate of HCC [5,6]. Therefore, prevention has become a primary strategy to reduce disease burden of liver cancer [7,8]. Specifically, chemoprevention is an essential way to confront HCC since antiviral agents cannot entirely abolish the risk of HCC in patients with cirrhosis, especially those caused by HCV infection [9]. The objective of chemoprevention is to impede, arrest or reverse the early phase of carcinogenesis or halt its progression to malignancy [10].

Abbreviations: HCC, hepatocellular carcinoma; IκBs, NF-κB inhibitory proteins; TrxR, thioredoxin reductase; Trx, thioredoxin; BS, butaselen; NAC, N-acetyl-L-cysteine; DEN, diethylnitrosamine; GPC3, glypican-3; COX-2, cyclooxygenase-2; iNOS, inducible nitric oxide synthase; SRB, sulforhodamine B; ROS, reactive oxygen species; TPA, phorbol ester

* Correspondence to: State Key Laboratory of Natural and Biomimetic Drugs, Department of Chemical Biology, School of Pharmaceutical Sciences, Peking University, No. 38 Xueyuan Road, Beijing 100191, PR China.
E-mail address: zenghh@bjmu.edu.cn (H. Zeng).
[1] The two authors contributed equally.

http://dx.doi.org/10.1016/j.redox.2017.09.014
Received 17 September 2017; Accepted 18 September 2017
Available online 22 September 2017

NF-κB/Rel family has been reported to connect chronic inflammation with carcinogenesis [11]. NF-κB is a hetero- or homodimer transcriptional factors and p50-p65 heterodimer is the most abundant form in mammals. NF-κB can be activated by phosphorylation and degradation of NF-κB inhibitory proteins (IκBs). Activated NF-κB translocating from cytoplasm to nucleus joins in regulation of transcription factors involved in inflammation, cell cycle progression, cellular survival and immune response [12]. In a prototype of HCC caused by cholestatic hepatitis, induction of IκB-super-suppressor inhibited the progression of transformed hepatocytes to HCC [11]. NF-κB activity has been demonstrated to be mediated by the activity of thioredoxin reductase (TrxR) in thioredoxin (Trx) system [13].

Trx system (Trx, TrxR and NADPH) plays a key role in maintaining redox balance, tumorigenesis and development [14]. Oxidized Trx could be reduced by TrxR with NADPH providing electron and Trx has protein disulfide reductase activity. Three isoforms of TrxR have been identified in mammals: TrxR1, TrxR2 and TrxR3. Serum TrxR level has also been recognized as a promising survival indicator in patients with HCC [15] and TrxR as a target of cancer prevention and treatment [16]. Butaselen (BS) is an organoselenium-containing compound designed to target TrxR.

In this study, we aim to explore the chemopreventive effect of BS against hepatocarcinogenesis and progression *in vivo* with a two-stage chemically induced HCC model and H22 hepatoma-bearing mouse model, and investigate its underlying mechanisms on cellular level.

2. Materials and methods

2.1. Chemicals

Butaselen (Fig. 1A, MW: 452 g/mol) was synthesized in the State Key Laboratory of Natural and Biomimetic Drugs, Peking University. Diethylnitrosamine (DEN) and CCl_4 were purchased from Sigma-Aldrich (St. Louis, USA). Ethanol was obtained from Hinbio, China. The NADPH oxidase inhibitor diphenyleneiodonium chloride (DPI) was purchased from Gene Operation (Michigan, USA). Mitochondria-targeted antioxidant mito-tempo (MT) was obtained from Santa Cruz (Texas, USA). Antioxidant N-acetyl-L-cysteine (NAC) was purchased from Sigma-Aldrich.

2.2. Cell culture and animals

The human HCC cell lines HepG2, Bel7402, Huh7 and murine HCC cell line H22 were purchased from Cell Resource Center at Peking Union Medical College (Beijing, China). Cells were cultured in DMEM (Macgene, China) supplemented with 10% fetal bovine serum (Excell Bio, China) and incubated at 37 °C with 5% CO_2.

Six-week-old male C57BL/6J mice (18–20 g) and four-week-old male Balb/c mice (16–18 g) were purchased from the Animal Center, Peking University Health Science Center. All animals were kept in standard laboratory conditions and provided with *ad libitum* food and water. The animal experiments were approved by the Research Ethics Committee of Peking University Health Science Center.

2.3. Measurement of chemopreventive effect of butaselen against hepatocarcinogenesis

Two-stage model of chemically initiated HCC was employed to assess the cancer preventive effect of BS following the schedule in Fig. 1B. C57BL/6J mice were randomly assigned into five groups: Control (n = 28), Model (n = 60), BSL (Model + 9 mg/kg BS, n = 40), BSM (Model + 18 mg/kg BS, n = 40), BSH (Model + 36 mg/kg BS, n = 40). Briefly, animals were given single dose of DEN (100 mg/kg, i.p.) at week 1. From day 3, animals were treated with 20% CCl_4 in olive oil (5 ml/kg, i.g.) twice a week by oral gavage. Then mice were given another injection of DEN (50 mg/kg, i.p.) at week 3 along with 10% ethanol solution as drinking water *ad libitum* simultaneously. The dosage of 20% CCl_4 was increased to 8 ml/kg twice a week from week 8, and 8 ml/kg thrice a week from week 12. Animals in control group were given solvent. BS was orally treated from week 0 to week 24, 6 times/week. Body weight were recorded every 14 days. Six mice were randomly sacrificed at week 6 and week 16 and ten mice at week 24. Serum and liver tissue samples were collected for further tests and pathological analyses.

2.4. Determination of in vivo tumor inhibitory effect of butaselen

In order to select a suitable dose for HCC treatment, Balb/c mice were randomly divided into 4 groups (control, BS 90 mg/kg, 180 mg/kg and 360 mg/kg, 6/group) and pretreated with 5‰ CMC-Na or BS for 3 days. Mice were injected subcutaneously with 10^6 H22 cells and BS were daily given by gavage. The weight and tumor volume were recorded every 3 days (volume = length × $(\text{width})^2$ × 0.5236).

To further validate the inhibitory effect of BS against HCC, 12 Balb/c mice were randomly assigned into two groups: control (5‰ CMC-Na, i.g., q.d., n = 6) and BS (180 mg/kg, i.g., q.d., n = 6). After three days of pre-treatment, mice were inoculated subcutaneously with 10^6 H22 cells and BS were daily administered. The inhibitory effects of BS on the growth of tumors developed from 10^5 or 10^4 H22 cells per mouse were studied simultaneously. Tumor volume was calculated every three days. Mice were sacrificed until tumor volume reached about 2000 mm^3 in the control group and serum was collected for analysis.

2.5. Histopathological and immunohistochemical analyses

The liver tissues were soaked in 4% paraformaldehyde for 24 h. After dehydrated and embedded in paraffin, 4 μm sections were cut for H & E and Masson staining. The pathological changes were assessed by an experienced pathologist who was blind to the treatments as Supplementary material Table S1. Immunohistochemical analysis with CD34 antibody (Abgent, USA) was conducted as standard procedures. Photos were taken with an optical microscope (Olympus, Japan).

2.6. Blood examination and liver function analysis

The mice blood test was conducted by Laboratory Animal Department of Peking University Health Science Center. ALT and AST analyses were assisted by Peking University Third Hospital. Alpha-foetoprotein (AFP) was measured with ELISA as instructions (Dingsheng Bio, China).

2.7. Enzymes activity assay

Determination of serum and intracellular TrxR, glutathione reductase (GR) and glutathione peroxidase (GPx) activity were practiced as described before [17].

2.8. Immunoblotting

Proteins were separated by SDS-PAGE and electrically transferred to PVDF membrane (Millipore, USA). The membrane was subsequently blocked by 5% non-fat milk at room temperature, followed by incubation with primary antibodies at 4 °C overnight, including β-actin (Santa Cruz Biotech., USA), Glypican-3 (GPC3), TrxR, TNF-α, IL-6, Cyclooxygenase-2 (COX-2), inducible nitric oxide synthase (iNOS, ProteinTech, China), CD34, Trx, pIκB-α and pNF-κB p65 (Abgent, USA). The membrane was incubated with HRP-conjugated secondary antibodies (Santa Cruz Biotech., USA), visualized with ECL detection reagent (Advansta, USA) and imaged by ChampGel 5000 Imager (Sagecreation, China).

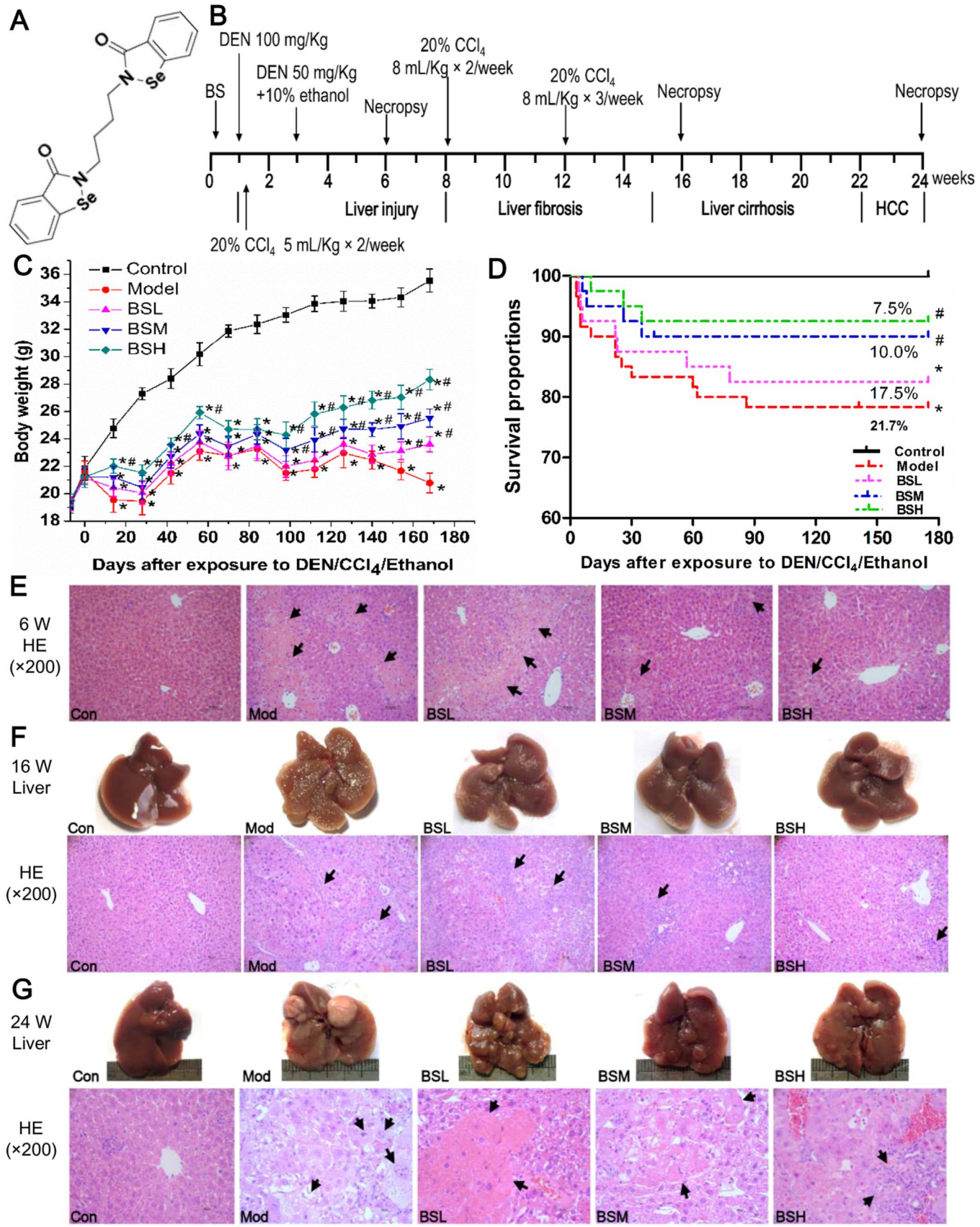

Fig. 1. Experimental schedule and preventative effect of butaselen against hepatocarcinogenesis. (A) Chemical structure of butaselen (BS). (B) Diethylnitrosamine (DEN), CCl_4 and 10% ethanol were used to induce model of hepatocellular carcinoma (HCC) for 24 weeks in C57BL/6J mice. Different doses of butaselen (BS) were administered in other three groups. (C) The body weight change and (D) survival proportions of mice in 180 days. (E) Representative hepatocellular damage at week 6. (F) Gross pathology and HE stain of cirrhosis at week 16. (G) Gross and pathological change of HCC at week 24. Data were shown as mean ± std, n ≥ 28 and analyzed with ANOVA or Log-rank test. *, $^{\#}$ $p < 0.05$ compared with control or model group. BSL, 9 mg/kg BS; BSM, 18 mg/kg BS; BSH, 36 mg/kg BS.

2.9. Reverse transcription-PCR (RT-PCR)

Total RNA was extracted with TRIzol reagent (Bioteke, China). 1 μg RNA was reverse-transcribed to cDNA according to the kit instruction (Thermo Fisher, USA). 20 μl reactions containing 2 × Taq PCR Master Mix (Tiangen, China) were adopted in DNA amplification. The primers were listed in Supplementary material Table S2. PCR products were electrophoresed with DuRed staining in 2% agarose gel. Images were recorded and analyzed by ChampGel 5000 Imager.

2.10. Cell viability assay

The sulforhodamine B (SRB) assay [18] was performed to measure the inhibitory effect of BS on the proliferation of HepG2, Bel7402 and Huh7 cells.

2.11. Lentiviral vector construction and cell transfection

The siRNA sequence targeting TrxR1 and a negative control were from Eriksson et al. [19], they are listed in Supplementary material Table S3 and synthesized by GenePharma (GenePharma, Shanghai, China). The lentivirus construction and plasmid packaging were performed as previously reported [20]. HepG2 cells were transfected with multiplicity of infections (MOIs) 20 with 5 μg/ml polybrene and selected with 1 μg/ml puromycin for 4 days.

2.12. Reactive oxygen species (ROS) measurement

Cells were exposed to 10 μM 2′,7′-Dichlorodihydrofluorescein diacetate (DCF-DA), which could be oxidized by H_2O_2, for 30 min at 37 °C after indicated treatments. Subsequently, cells were collected with 0.25% trysin-EDTA, washed twice with PBS and filtered through membrane before fluorescence at 340 nm could be measured by flow cytometer (BD FACSCalibur, USA). Dihydroethidium (DHE, Kaiji, China), another oxidative fluorescent dye was adopted to evaluate superoxide anion ($O_2^{\cdot-}$) production after BS treatment as previously described [21].

2.13. Assay of glutathione (GSH) and glutathione disulfide (GSSG) levels

HepG2 cells were exposed to BS for 24 h before protein extraction with NP-40 lysate added with sulfosalicylic acid to prevent loss of GSH. The assay measured GSH and GSSG were conducted as previously reported [22].

2.14. Annexin V/PI assay

Cells were collected and stained with Annexin V/PI (Biosea, China) following the manufacturer's instructions. Apoptotic cells were examined using a flow cytometer.

2.15. Cell cycle analysis

Cells after BS treatment were harvested and fixed in 70% ethanol at −20 °C overnight. Cells were incubated with RNase and stained with PI before analyzed by the flow cytometer.

2.16. Immunofluorescence imaging

Cells were washed twice with ice-cold PBS and fixed with 4% paraformaldehyde. After permeabilizaiton with 0.2% Triton X-100, cells were blocked with 1% BSA and incubated with Trx antibody (Abgent, USA) at 4 °C overnight. After PBS rinsing and incubation with secondary antibody, nuclei were visualized by DAPI staining. Images were obtained using a confocal microscope (Nikon A1, Japan).

2.17. Statistical analysis

Data collected from at least three independent experiments were expressed as mean ± standard deviation. One-way ANOVA was used to assess statistical differences. Log-rank test was used to compare survival and length of tumor formation between groups. $P < 0.05$ was considered statistically significant.

3. Results

3.1. Butaselen protects mice from developing hepatocellular carcinoma

At the beginning of DEN/CCl_4/ethanol administration, mice in the model and BS treatment groups were lean, dispirited and their fur was lusterless; however, the body conditions of mice in BS treatment groups gradually improved and became active. Fig. 1C shows that body weight of mice in control group continuously increased from 19 g to approximately 35 g, while the weight of model group fluctuated and were only 1.09 fold of initial weight at the end of experiment. The mice in BS groups were relatively resistant to dosage increase of 20% CCl_4 from 5 ml/kg to 8 ml/kg at week 8 and frequency raising from twice/week to 3 times/week at week 12, thus their body weight were dose-dependently higher than that in model group. Cumulatively, 21.7% (13/60) mice in the model group died after 24 weeks, while the death rate was 17.5% (7/40), 10.0% (4/40) and 7.5% (3/40) respectively in BSL, BSM and BSH groups, with significant reduction in BSM and BSH group compared with model group (Fig. 1D).

BS treatment could impede chronic hepatocellular damage. The livers in model group after 6-weeks exposure to DEN/CCl_4/ethanol were swollen and the surface was coarsely covered with little granule. While in BS treatment groups, liver volumes were smaller than the model group and fewer granules were observed. The H & E staining showed normal cellular architecture in all the control groups (Fig. 1E–G). After 6 weeks, hepatocellular edema, ballooning degeneration and confluent necrosis connecting portal field to central vein accompanied by sporadic neutrophils infiltration were observed in model group; after BS treatment, hepatocellular necrosis and inflammation were significantly ameliorated, especially in BSH group (Figs. 1E and 2A). The levels of serum ALT and AST also reflected the protective effect of BS treatment against hepatocellular damage (Fig. 2B).

BS treatment could protect mice from developing fibrosis and cirrhosis. At the week 16, mice liver in model group turned yellowish-tan with diffuse uniform micronodules separated by fibrous septa. Steatosis, severe centrilobular necrosis, porto-portal and porto-central bridging fibrosis, rearrangement of blood circulation and pseudolobule with macrophage infiltration were observed in the model group. After BS treatment, liver gradually regained red color and number of nodules was declined; inflammation, hepatocellular necrosis and fibrosis were lessened in a dose-dependent manner (Figs. 1F and 2C). Masson staining showed collagen fibers formed in porto-portal and porto-central areas in model group, which were significantly reduced after BS treatment (Fig. 2D).

BS treatment could reduce murine HCC incidence without immunosupression. At week 24, HCC formation rate in model group was 80% (Table 1), hepatic gray nodule were developed varying from 0.1 to 0.8 cm in diameter; normal liver lobule destruction, altered hepatic foci, hepatocellular edema, steatosis and marked nuclear polymorphism in H & E staining were seen in model group (Fig. 1G). The HCC formation rate, number of gray nodules, hepatic lobule damage and hepatocellular dysplasia were significantly ameliorated by BS administration (Table 1, Figs. 1G and 2E). At necropsy, thymus in model group was markedly atrophied compared with control group, spleen was remarkably swollen; WBC, RBC and PLT were about 2.1, 0.9 and 0.7 fold of those in control group, indicating chronic inflammation and immunological suppression after long-term DEN/CCl_4/ethanol exposure (Table 1). Liver/body weight, spleen/body weight and WBC were

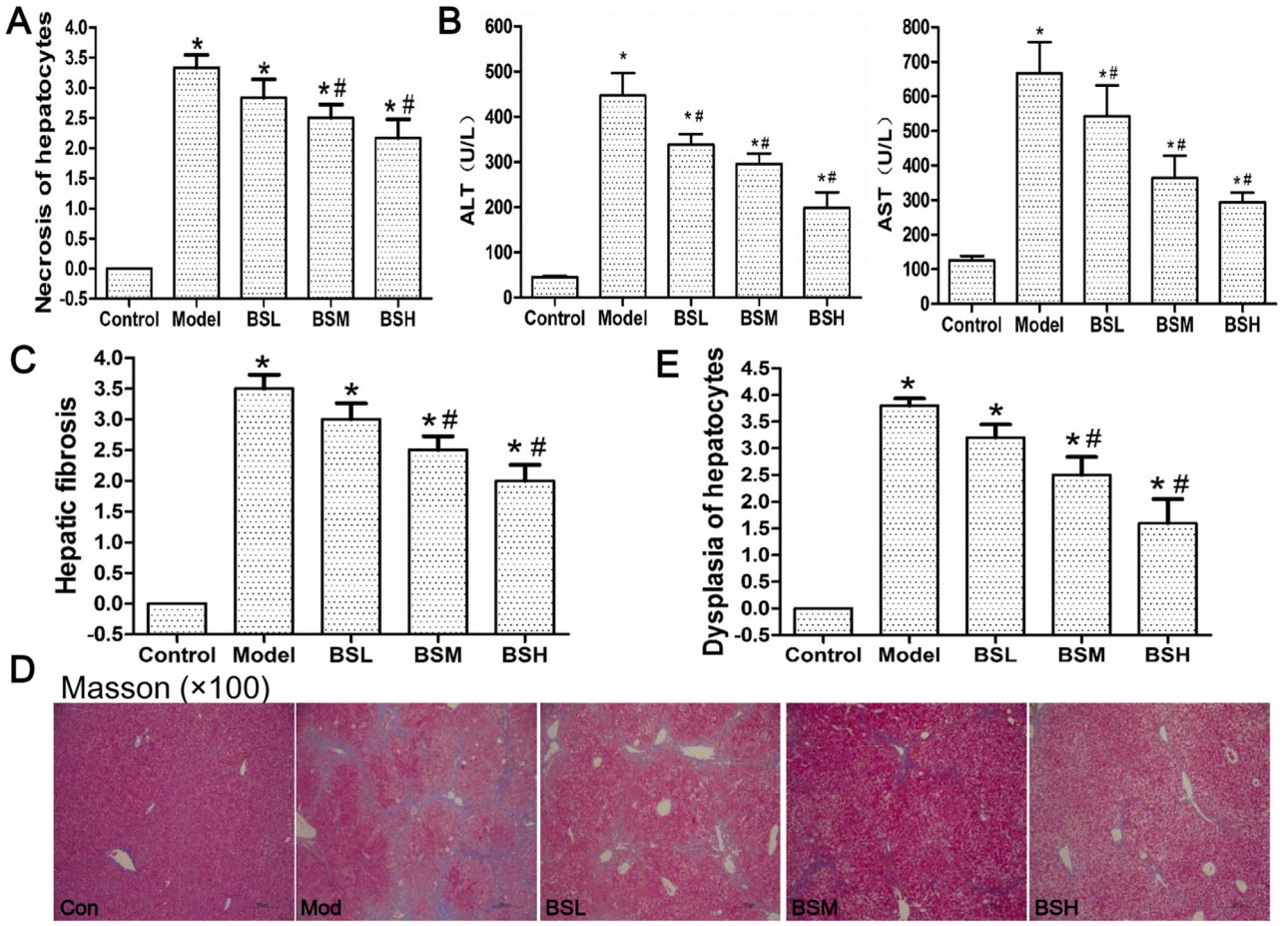

Fig. 2. Biomarkers and pathological changes during hepatocarcinogenesis. (A) Histogram analysis of necrosis grade of hepatocytes at week 6. (B) Serum ALT and AST levels at week 6. (C) Statistical analysis of hepatic fibrosis grade and (D) Masson stain of mice liver tissue at week 16. Collagen is in blue color. (E) Histogram analysis of hepatocellular dysplasia grade at week 24. Data were shown as mean ± std, n ≥ 6 and analyzed with ANOVA. *, # $p < 0.05$ compared with control or model group. BSL, 9 mg/kg BS; BSM, 18 mg/kg BS; BSH, 36 mg/kg BS.

significantly attenuated after BS treatment; meanwhile, thymus/body weight, RBC and PLT were improved, showing that BS positively regulated the immunological functions.

Recognized markers for HCC including GPC3, CD34 and serum AFP were measured at week 24. Immunohistochemical analysis showed that CD34 was diffusely expressed in model group, and the expression was gradually declined upon BS treatment. The expression of GPC3 and CD34 from mice liver were elevated in model group and dose-dependently attenuated in BS groups (Fig. 3A, Supplementary material Fig. S1A and B). AFP was approximately 4.1 fold in model group compared with control group and was reduced to normal level under BSH treatment (Fig. 3B). TrxR activity were markedly elevated from 13.1 U/mg in control group to 70.7 U/mg in model group and was significantly reduced to 57.0, 36.7 and 22.7 U/mg respectively in BSL, BSM and BSH groups (Fig. 3C). TrxR and Trx expression were raised in model group and were remarkably attenuated by BS treatment (Fig. 3D, Supplementary material Fig. S1C and D), indicating that BS may prevent hepatocarcinogenesis through TrxR and Trx inhibition. As NF-κB pathway plays an essential role connecting inflammation and cancer, pIκB-α and pNF-κB p65 expression were explored in this study, which were also enhanced in model group and lowered by BS in dose-dependent manner, indicating that NF-κB pathway was activated during hepatocarcinogenesis and could be suppressed by BS (Fig. 3D, Supplementary material Fig. S1E and F). NF-κB activation was previously reported to upregulate expression of inflammatory factors [12], in our study, the gene and protein levels of TNF-α, IL-6, COX2 and iNOS were significantly improved in model group, demonstrating their role in the process of hepatocarcinogenesis (Fig. 3E and F, Supplementary material Fig. S2). Consistently, the above inflammatory factors upregulation under DEN/CCl_4/ethanol exposure were also attenuated by BS treatment.

Table 1
The HCC rate and nontoxicity of butaselen in mice models at the 24th week.

Groups	No.	HCC (%)	Liver/body weight (%)	Thymus/body weight (%)	Spleen/body weight (%)	WBC (× 10^9/L)	RBC (× 10^{12}/L)	PLT (× 10^9/L)
Control	10	0	5.17 ± 0.22	0.25 ± 0.02	0.27 ± 0.06	7.10 ± 1.52	9.76 ± 0.55	685.40 ± 37.58
Model	10	80	8.18 ± 0.39*	0.13 ± 0.04*	0.54 ± 0.12*	15.20 ± 3.73*	8.34 ± 0.41*	506.60 ± 57.40*
BSL	10	40	7.03 ± 0.53*#	0.16 ± 0.03*	0.44 ± 0.11*	13.26 ± 3.4*	9.06 ± 0.12	523.40 ± 38.96*
BSM	10	20	6.18 ± 0.46*#	0.19 ± 0.03*#	0.32 ± 0.07#	12.78 ± 3.06*	9.13 ± 0.36	615.50 ± 34.29#
BSH	10	10	5.65 ± 0.38#	0.22 ± 0.04#	0.29 ± 0.04#	9.80 ± 1.82#	9.15 ± 0.62#	631.40 ± 25.22#

Data were shown as mean ± std, n ≥ 6 and analyzed with One-way ANOVA. *, # $p < 0.05$ compared with control group or model group. BSL, 9 mg/kg BS; BSM, 18 mg/kg BS; BSH, 36 mg/kg BS. WBC, white blood cells; RBC, red blood cells; PLT, platelet.

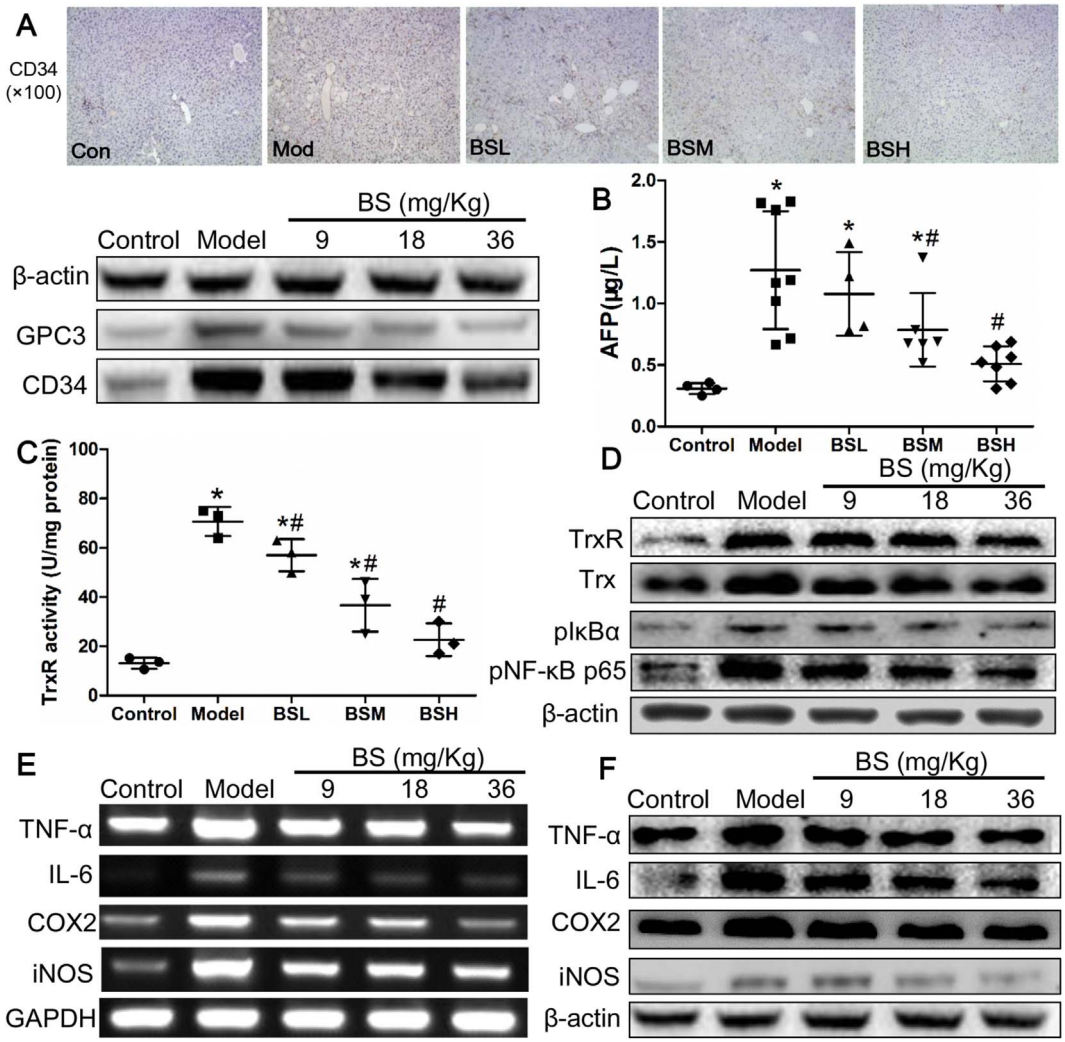

Fig. 3. The biomarkers change and underlying mechanisms of butaselen (BS) to prevent hepatocarcinogenesis. (A) Histoimmunochemical and immunoblotting analysis of glypican-3 (GPC3) and CD34. Serum level of (B) alpha-fetal protein (AFP), and (C) thioredoxin reductase (TrxR) activity at week 24. (D) Protein expression of TrxR and NF-κB pathway in liver of every group. (E) Gene and (F) protein level of inflammatory factors in mice liver. Data were shown as mean ± std, n ≥ 6 and analyzed with One-way ANOVA. *, # $p < 0.05$ compared with control or model group.

3.2. Butaselen halts progression of hepatocarcinoma in mice models

To investigate an effective dose of BS to inhibit HCC growth *in vivo*, 90, 180 and 360 mg/Kg BS were administered to murine models injected with 1×10^6 H22 cells. The tumor sizes in the groups of 180 and 360 mg/Kg BS treatment were significantly smaller than that in the control group from the 9th day (Fig. 4A). Overall, BS showed a dose-dependent inhibitory effect towards tumor volume in H22 tumor bearing mice model (Fig. 4A and B) and we selected 180 mg/Kg BS for further experiments. The body weight, ratios of organ to body weight and WBC in the BS treatment groups were not significantly different from the control group (Table 2).

1×10^4–1×10^6 H22 cells were inoculated in Balb/c mice, with the number of H22 cells declined, tumor volumes in the 180 mg/kg BS group were much smaller than control groups (Fig. 4C and D). At the end of experiment, the inhibitory rate of tumor volumes in BS treatment group was 49.26%, 60.94% and 92.29% respectively in the groups implanted 1×10^6, 1×10^5 and 1×10^4 H22 cells per animal. In addition, BS treatment significantly prolonged time needed for tumors to reach 100 mm^3 (Fig. 4E). With 1×10^4 H22 cells implantation in the control group, all mice developed tumor at day 12, while in the BS treatment group, only 50% (3/6) mice developed tumors larger than 100 mm^3 at day 21.

3.3. Butaselen induces G2/M arrest and apoptosis in hepatocellular carcinoma cells by inhibiting TrxR activity

As displayed in Fig. 5A, BS inhibited the proliferation of HCC cell lines Bel7402, HepG2 and Huh7 in a dose- and time-dependent manner. The IC_{50} values of the three cell lines were shown in Table 3. Due to relatively high TrxR1 expression and activity (Fig. S3A), HepG2 cells were used for subsequent studies.

It was observed that HepG2 cells in G2/M phase were significantly augmented as BS concentration increased (Fig. 5B). Besides, BS treatment dose-dependently induced early and total apoptosis in HepG2 cells (Fig. 5C).

To explore the anti-proliferation mechanisms, intracellular ROS levels were evaluated. The fluorescent probes DCF-DA and DHE reacted with H_2O_2 and superoxide respectively were used. DCF fluorescence intensity was dose-dependently increased by BS, while reduced markedly by pretreatment of antioxidant NAC (Fig. 6A). Likewise, the DHE fluorescence intensity was elevated with 30–40 μM BS treatment and decreased by NAC. The unstable nature of superoxide, which could be rapidly converted to H_2O_2, may account for the relatively minor elevation of DHE fluorescence intensity compared with DCF after BS treatment [23]. Besides, the ratio of intracellular GSH to GSSG, another ROS production marker, was significantly decreased (Fig. 2B). In a

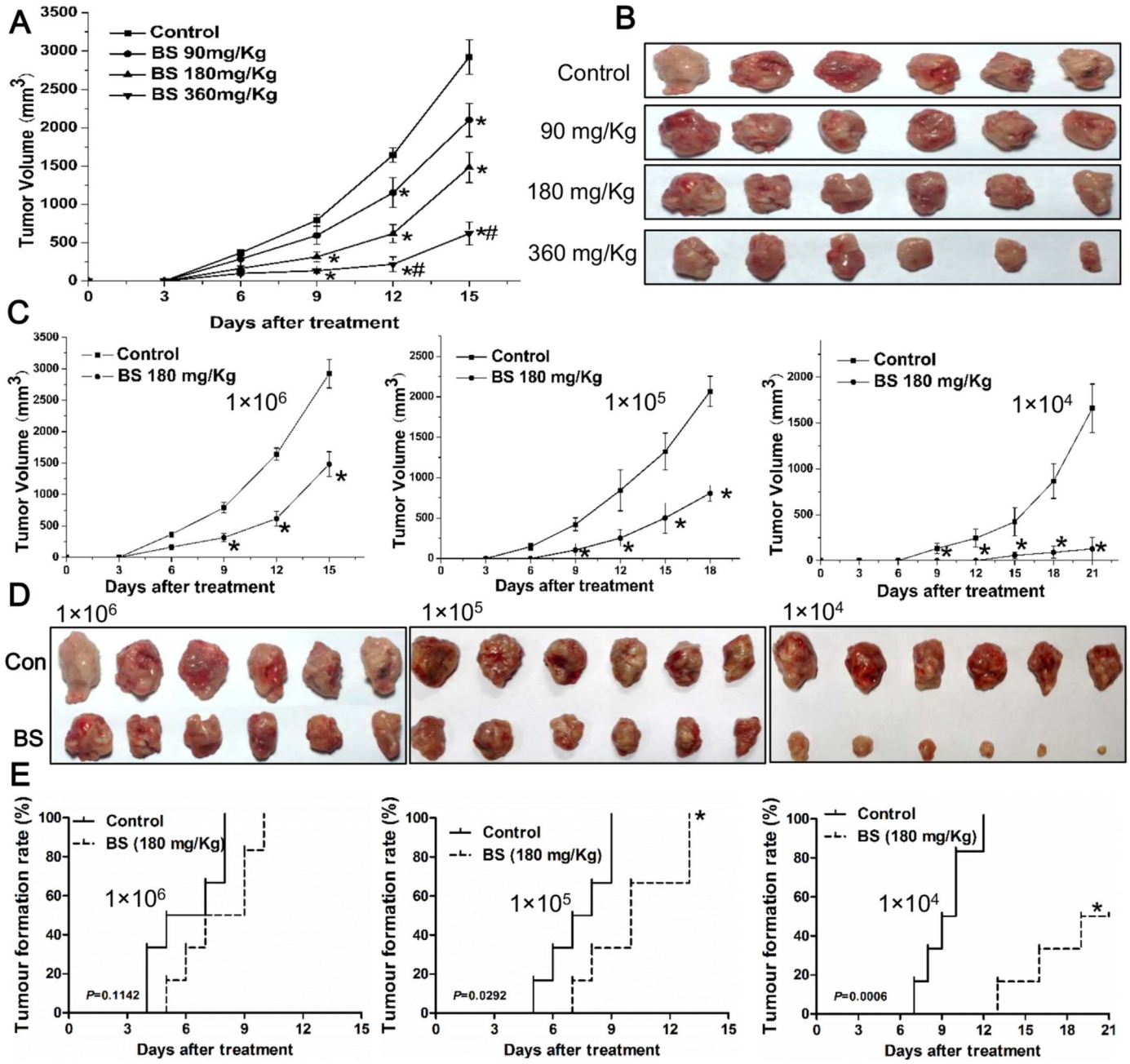

Fig. 4. The *in vivo* inhibitory effect of butaselen (BS) on hepatocellular carcinoma (HCC). (A) The tumor volume changes and (B) gross pathology of H22 mice models injected with 1 × 10^6 cells after BS treatments. (C) Tumor volume analysis, (D) Gross pathology and (E) HCC formation rate in control or 180 mg/kg BS treatment mice models implanted with 1 × 10^4–1 × 10^6 H22 cells. Data were shown as mean ± std, n = 6, analyzed with One-way ANOVA and Log-rank test. *, # $p < 0.05$ compared with control or BS 180 mg/kg group.

consequence, NAC significantly reduced the BS inhibition on HepG2 cells (Fig. 6C). In the anti-oxidant system, GPx could reduce H_2O_2 to water with GSH oxidized to GSSG and GR would reduce GSSG back to GSH; peroxiredoxin, one of the substrates of Trx which could be reduced by TrxR, could convert H_2O_2 to water as well [23]. Therefore, the intracellular activities of TrxR, GPx and GR were measured. TrxR activity of HepG2 cells was inhibited by 14.55%, 35.70% and 66.78% respectively after 20, 30 and 40 μM BS treatment for 24 h; the

Table 2
The nontoxicity of butaselen in mice transplanted with 1 × 10^6 H22 cells.

Groups	No.	Body weight (g)	Liver/body weight (%)	Thymus/body weight (%)	Spleen/body weight (%)	WBC (× 10^9/L)
Control	6	32.36 ± 1.32	5.07 ± 0.93	0.17 ± 0.05	0.63 ± 0.11	9.80 ± 3.03
BS 90 mg/kg	6	31.02 ± 2.67	5.23 ± 0.48	0.19 ± 0.03	0.67 ± 0.14	10.20 ± 2.06
BS 180 mg/kg	6	30.86 ± 1.83	5.19 ± 0.56	0.17 ± 0.04	0.60 ± 0.12	9.95 ± 2.75
BS 360 mg/kg	6	30.59 ± 0.84	5.13 ± 0.98	0.18 ± 0.05	0.62 ± 0.14	9.70 ± 1.69

Data were shown as mean ± std, n = 6 and analyzed with One-way ANOVA. BS, butaselen; WBC, white blood cell.

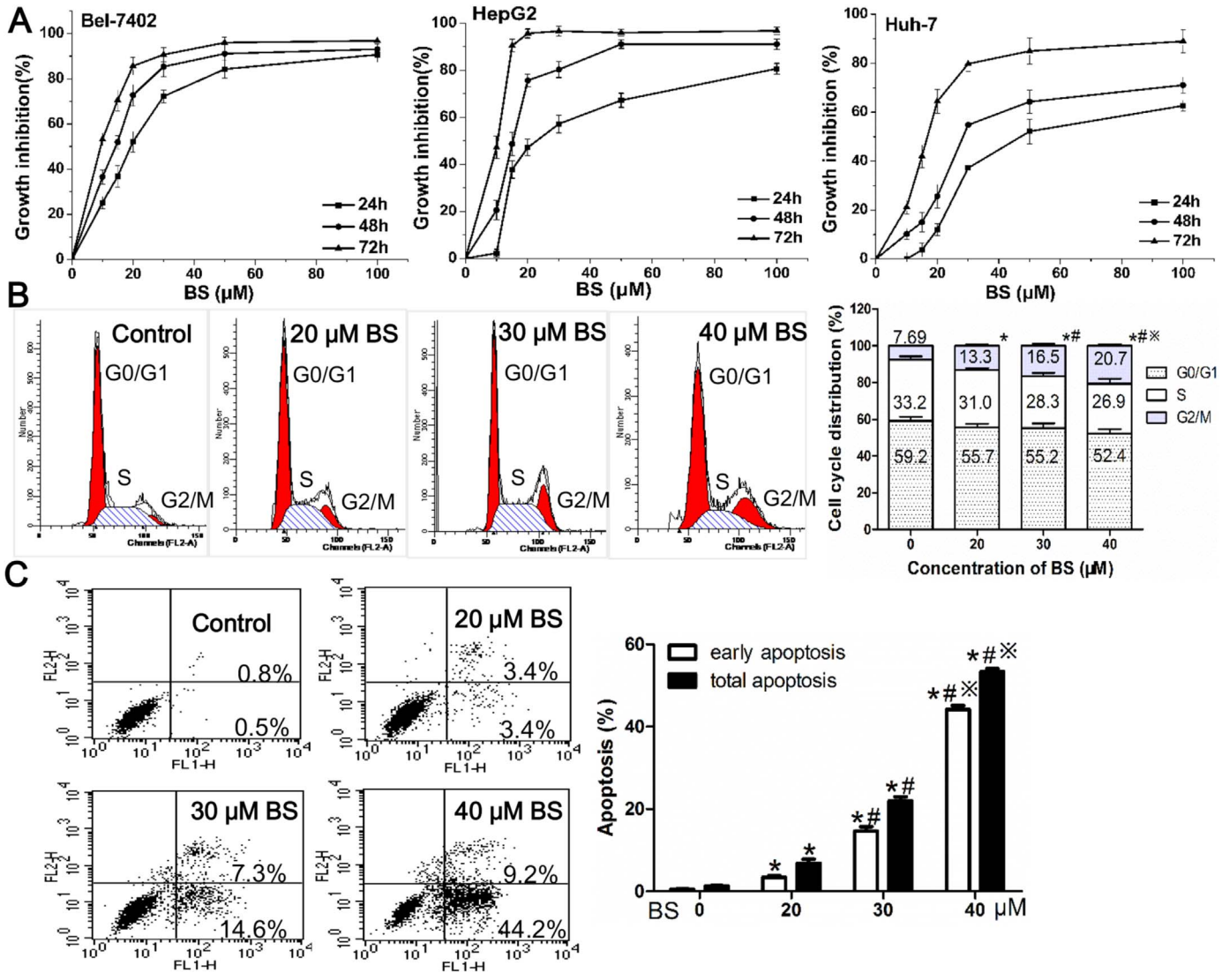

Fig. 5. Proliferative inhibition, G2/M arrest and apoptosis in hepatoma cells induced by BS treatment. (A) Dose- and time-dependent inhibition of BS on Bel7402, HepG2 and Huh7 cells after 24–72 h treatment. (B) Representative figure and histogram analysis of G2/M arrest in HepG2 cells after 20–40 μM BS treatment for 24 h. (C) Annexin V-PI analysis and statistical analysis of early and total apoptosis rate after BS treatment for 24 h on HepG2 cells. Data were shown as mean ± std, n ≥ 3 and analyzed with One-way ANOVA. $^{*, \#, ※}$ $p < 0.05$ compared with control group, 20 μM BS group or 30 μM BS group.

corresponding HepG2 growth inhibition rate was 31.05%, 57.83% and 71.62% (Fig. 6D), which was in high consistency with TrxR activity decrement. However, the GPx activity were slightly increased under high ROS conditions and GR activity almost remained unchanged, which was in consistence with GSH/GSSH decrement. To validate the role of TrxR in maintaining intracellular redox balance, HepG2 cell line stably expressing low levels of TrxR1 was established by using shRNA (Fig. 6E). TrxR activity in LV-TR1-shRNA transfected cells were decreased about 75% compared with control cells (Fig. 6E). Consequently, ROS was markedly higher after TrxR1 knockdown in HepG2 cells (Fig. 6E). In order to confirm the source of ROS, DPI and MT which were inhibitors of NADPH oxidase and mitochondrion, were pretreated before 40 μM BS. Surprisingly, MT did not affect ROS level induced by BS; on the contrary, DPI significantly reduced the ROS (Fig. 6F).

TrxR1 knockdown led to slower proliferation and increased resistance to BS treatment compared with LV-NC-shRNA and HepG2 cells (Fig. 7A and B). As a substrate of TrxR1, the expression of Trx was explored and found to be significantly lowered by BS treatment dose-dependently, which was verified by immunofluorescence, RT-PCR and immunoblotting (Fig. 7C–E, Supplementary material Fig. S3B),

Table 3
Proliferation inhibition of butaselen against hepatocellular carcinoma cells.

Time (h)	Bel7402		HepG2		Huh7	
	IC_{50} (μmol/L)	MI (%)	IC_{50} (μmol/L)	MI (%)	IC_{50} (μmol/L)	MI (%)
24	20.01 ± 0.45	90.68	25.49 ± 0.59	80.68	48.21 ± 0.57	62.68
48	14.26 ± 0.35	93.10	16.25 ± 0.30	91.10	27.37 ± 0.51	71.10
72	8.32 ± 0.39	96.83	10.26 ± 0.45	96.83	18.92 ± 0.46	89.00

Data were shown as mean ± std, n ≥ 3 and analyzed with One-way ANOVA. MI, maximum inhibition rate.

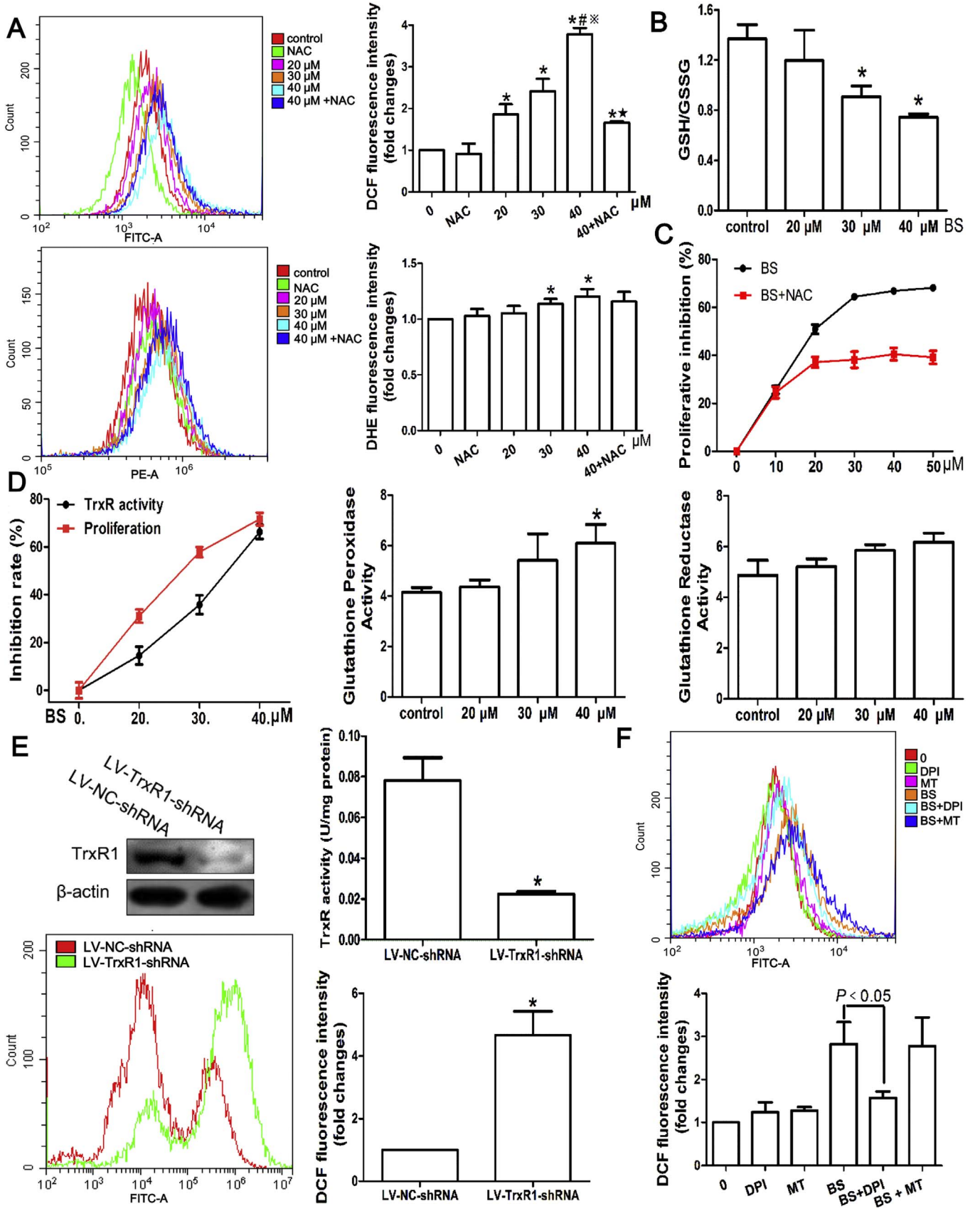

(caption on next page)

Fig. 6. ROS production mediated by TrxR activity inhibition after butaselen (BS) treatment for 24 h. (A) Representative histogram plot and statistical analysis of ROS stained by DCF-DA and DHE. Pretreatment of antioxidant N-acetyl-L-cysteine (NAC, 5 mM) decreased ROS level induced by BS. (B) The ratio of glutathione (GSH) to glutathione disulfide (GSSG) was markedly reduced after BS treatment. (C) Proliferative inhibition was significantly lower of BS added with 5 mM NAC compared with BS alone. (D) TrxR activity inhibition were generally in parallel with proliferative inhibition of HepG2 cells. Glutathione peroxidase and glutathione reductase activities were to some extent elevated. (E) Significantly lower TrxR1 expression, TrxR activity and higher ROS level after HepG2 cells transfected with LV-TrxR1-shRNA compared with LV-NC-shRNA. (F) The ROS induced by 40 μM BS was inhibited by NADPH oxidase inhibitor DPI. Data were shown as mean ± std, n ≥ 3 and analyzed with One-way ANOVA. $^{*, \#, ※, ★}$ $p < 0.05$ compared with control group, 20 μM BS group, 30 μM BS group or 40 μM BS group. DPI, diphenyleneiodonium chloride; MT, mito-tempo.

indicating that BS not only inhibited TrxR activity, but also decreased its substrate Trx expression, disrupting intracellular redox balance.

It has been reported that transcription factor AP-1 plays an important role in regulating proliferation, apoptosis and cell cycle *etc.* [24], while the DNA binding activity of AP-1 is regulated by Ref-1. In our study, the gene and protein expression of Ref-1 were also significantly attenuated after BS exposure (Fig. 7D and E, Supplementary material Fig. S3C), indicating the involvement of Trx/Ref-1/AP-1 pathway in G2/M arrest. Gene and protein levels of cyclin B1 and CDK1, which form a complex to propel cells to go through mitosis phase, were examined and found to be remarkably decreased upon BS treatment (Fig. 7D and E, Supplementary material Fig. S3D and E).

Expressions of NF-κB and mitochondrial apoptosis pathway were measured to explore the mechanisms controlling apoptosis. The pIκB-α and pNF-κB p65 expression after 24 h BS treatment were significantly decreased (Fig. 7F, Supplementary material Fig. S4A and B). The Bcl-2/Bax ratio of both mRNA and protein were significantly diminished; in addition, pro-Caspase-3 was dose-dependently attenuated by BS treatment (Fig. 7G and H, Supplementary material Fig. S4C and D).

4. Discussion

We found that BS treatment was able to prevent hepatocarcinogenesis and progression in mice models. The initiation and promotion of two-stage chemically induced rodent model of HCC can effectively simulate the injury-fibrosis-malignancy pathological process observed in human hepatocarcinogenesis, thus it has become a well-recognized animal model to study the prevention and therapy of HCC [25]. DEN,

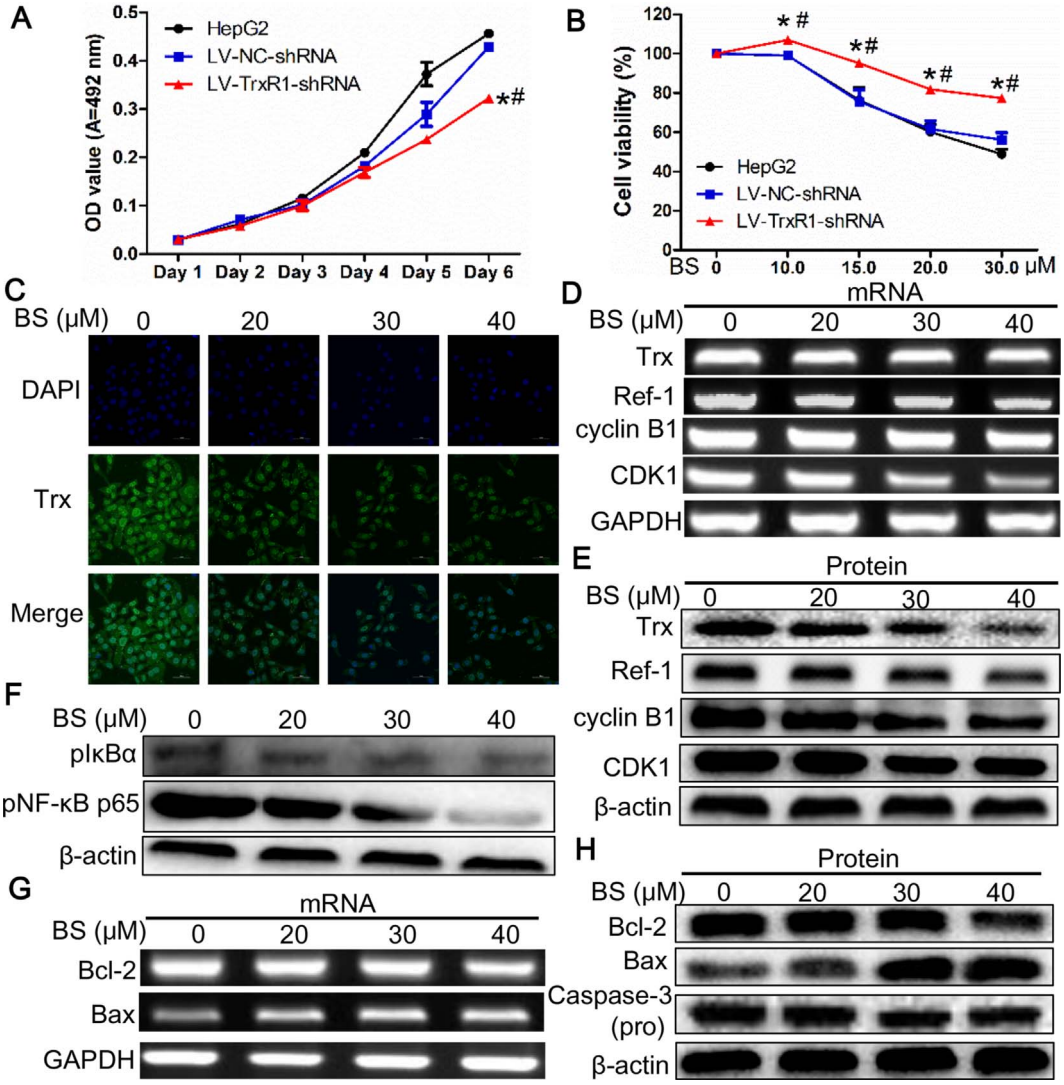

Fig. 7. The effects of TrxR1 knock down on proliferation, viability and mechanisms mediating G2/M arrest and apoptosis of HepG2 cells (A) Knock-down of TrxR1 inhibited HepG2 cells proliferation and (B) increased resistance to BS treatment. (C) Immunofluorescent analysis of Trx level upon BS treatment. (D) Gene and (E) protein levels of Trx, Ref-1 and molecules mediating G2/M arrest. (F) Downregulation of NF-κB pathway. Level of (G) mRNA and (H) proteins mediating mitochondria-dependent apoptosis. Data were shown as mean ± std, n ≥ 3 and analyzed with One-way ANOVA. $^{*, \#}$ $p < 0.05$ compared with control or LV-NC-shRNA group.

used as a tumor initiator, can dose-dependently alkylates DNA structures and produce ROS which lead to protein, lipid and DNA damage [26]. CCl_4 can be metabolized to damage membrane and promote Kupffer cells to secret proinflammatory factors such as TNF-α and IL-6 [27], thus served as a promoting agent along with ethanol to trigger HCC. In consistence with previous report [25], the mice in the model group could not tolerate acute and chronic liver toxicity or lung infection induced by DEN/CCl_4, causing dropped body weight (Fig. 1C), 21.7% of which even died after 90 days (Fig. 1D). The severe damage of DEN/CCl_4/ethanol to liver was manifested by the elevation of ALT and AST after 6 weeks exposure in the model group, which were enhanced by 10 and 5 folds respectively compared to control group (Fig. 2B). When hepatocytes injury occurs, ALT and AST could be released from cytoplasm and mitochondrion into extracellular space and circulation, leading to the elevation of serum ALT and AST.

Based on the histopathological analysis, it is noted that chronic injury, liver fibrosis and HCC established after chemicals exposure could be significantly ameliorated by BS treatment (Figs. 1E–G, and 2). The H & E staining showed that hepatocellular damage, inflammation, fibrosis, cirrhosis and dysplasia in mice liver were remarkably improved by BS treatment, resulting in a significant decrease of liver/body weight and HCC formation rate (Table 1). The HCC rate declined from 80% in the model group, which was similar to the data reported by Luo et al. [25], to 40%, 20% and 10% respectively in BSL, BSM and BSH groups. Furthermore, in the hepatoma-bearing mouse model under 1×10^4 H22 cells injection, 50% mice did not developed tumors larger than 100 mm^3 after 180 mg/kg BS treatment for consecutive 21 days and the tumor volumes were reduced by 92.29% compared with control group (Fig. 4C–E). As the number of implanted H22 cells decreased, BS treatment showed stronger inhibition of HCC development and progression, indicating that once tumor cells appear *in vivo*, BS should be administered as early as possible to achieve maximal chemopreventive effect. However, the exact inhibitory rate of BS from the stage of cirrhosis to HCC is unclear, since BS inhibited hepatocarcinogenesis from the initiation of chronic inflammation. For patients, the development from cirrhosis to HCC takes only a few years, thus it is critical to intervene progression at the cirrhosis stage. So far, anti-viral regimes are not able to abate HCC risk in patients with cirrhosis infected with HCV [28], and further studies can focus on whether BS can retard cirrhosis progressing into HCC.

BS treatment on one hand could reduce a panel of biomarkers of HCC (AFP, GPC3 and CD34). On the other hand, it exhibited very low toxicity in mice models. GPC3 is mainly expressed in HCC tissue, but not in other liver diseases or cancers [29]. CD34, an endothelial cell marker, has also been proved to predict prognosis in patients with HCC [30], and can be combined with GPC3 to differentiate HCC from benign hepatic nodules [31]. In our study, AFP, GPC3 together with CD34 were adopted to improve the sensitivity and specificity of HCC diagnosis in mice models after chemicals exposure, and their decrement after BS treatment (Fig. 3A and B) reflected that BS could effectively inhibit hepatocarcinogenesis. At the same time, the general physical conditions of mice in BS treatment groups were much better than those in the model group during the experiment. The significantly higher body weight and lower death rate in BS treatment groups supported that BS treatment could partly counteract the long-term toxicity of DEN/CCl_4/ethanol (Fig. 1C and D). The ratio of thymus to body weight was dose-dependently increased back to 0.22 ± 0.04% after BS treatment, which was not significantly different from 0.25 ± 0.02% in control group (Table 1). Likewise, the number of RBC and PLT were also augmented after BS treatment, neutralizing poisonousness of DEN/CCl_4/ethanol. Furthermore, in the H22-bearing mouse model, BS brought substantial reduction in terms of tumor volume while showed little influence on the body weight, organs/weight and WBC (Table 2). The above results showed that BS could effectively prevent hepatocarcinogenesis through intercepting all stages, namely chronic inflammation, fibrosis, cirrhosis and tumor progression without suppressing immunological functions of mice models, indicating that BS could potentially be used as HCC chemopreventive agent.

BS treatment inhibited the TrxR and NF-κB pathway *in vivo* and *in vitro*. Kumar et al. reported that tumor promoters (phorbol ester (TPA) and others) would enhance activity of both Trx and TrxR in mice epidermis [32]. Trx mRNA in human lymphocytes was increased by TPA, and Trx can be secreted into medium [33]. During hepatocarcinogenesis, DEN produce ROS and Trx system was activated to lessen oxidative damage (Fig. 3C and D). Long-lasting activation of Trx system would lead to cellular proliferation, apoptotic evasion, sustained angiogenesis and invasion, which ultimately result in malignancy [16]. Therefore, mitochondrial TrxR2 were found to overexpress in human HCC tumor tissues compared with adjacent normal tissues [34]. Besides, the TrxR1 activity in cytosol was increased 3.5 fold and mRNA of TrxR in nodules was significantly higher than normal rat liver in chemically-induced liver nodules of rats [35]. He et al. proved that BS could decrease activity of rat liver TrxR *in vitro* [36]. In our study, liver tissue and intracellular TrxR activity were dose-dependently decreased by BS treatment and in high consistence with proliferative inhibition (Figs. 3C and 6D). The higher proliferative inhibition may be a result of an enlargement of TrxR activity inhibition, since trx could reduce a broad of substrates, including peroxiredoxin, ribonucleotide reductase and ASK-1 and so on [14]. After TrxR1 was inhibited by BS or downregulated by shRNA, the intracellular ROS of HepG2 cells were significantly elevated (Fig. 6A and E), demonstrating an essential role of TrxR1 in regulating redox homeostasis. Consistent with our results, Zhang et al. also revealed that serum TrxR activity of mice HCC models were highly elevated and can be decreased by TrxR inhibitors (auranofin or cisplatin) [37]. We also found that TrxR and Trx expression were down-regulated by BS treatment both *in vivo* and *in vitro* (Figs. 3D and 7C–E). The decrement of TrxR and Trx are known to mediate a series of redox-dependent proteins, including NF-κB and Ref-1 [16]. IκBα usually integrates with NF-κB and stops NF-κB from translocating into nucleus. Previous report proved that two conserved serine residues in N-terminal of IκBα are phosphorylated and gets degraded once cells are stimulated, thus NF-κB is released and activated [12]. Hence in our study, the pIκBα and pNF-κB p65, representing the active state, were also investigated and found to increase in model group and decrease after BS treatments, proving that NF-κB pathway was activated during hepatocarcinogenesis and could be inhibited by BS (Figs. 3D and 7F).

BS treatment could impede hepatocarcinogenesis through anti-inflammation. In our study, the gene and protein expression of proinflammatory factors TNF-α, IL-6, COX-2 and iNOS in liver tissue were gradually diminished by BS treatments (Fig. 3E and F). In hepatic stellate cells (HSC), TNF-α and IL-6 secreted by Kupffer cells will activate intracellular NF-κB pathway, resulting in increased HSC survival, fibrogenesis and cirrhosis [38]. COX-2, the rate-limiting enzyme to produce prostanoids, plays vital roles in inflammation and correlated with key molecules in hepatocarcinogenesis (VEGF, p-Akt and iNOS *etc.)* [39]. The COX-2 inhibitor celecoxib has been proved by FDA to prevent familial adenomatous polyposis. iNOS catalyzes nitric oxide production, which enhances oxidative DNA damage, inhibits DNA repair and cellular apoptosis; combined negative iNOS and COX-2 expression significantly improved survival in patients with HCC [40]. Furthermore, the anti-inflammatory effect of BS was echoed by the WBC number decrement in BS groups (Table 1). Meanwhile, the ratio of liver and spleen to body weight were remarkably decreased by BS treatment compared with model group. The above results demonstrated that BS could inhibit TrxR/NF-κB/proinflammatory factors to achieve anti-inflammation and hepatocarcinogenesis prevention.

To confirm that BS induce ROS through inhibiting TrxR, an *in vitro* TrxR1-knockdown HepG2 cell line was established by RNA interference (Fig. 6E). LV-TR1-shRNA cells exhibited significantly lower TrxR activity, higher ROS level and diminished proliferative rate compared with LV-NC-shRNA cells (Figs. 6E and 7A), which were similar to the inhibition of HepG2 cells after BS administration. Furthermore, the cell

viability was markedly higher in LV-TR1-shRNA cells after treated with BS compared with HepG2 and LV-NC-shRNA cells (Fig. 7B), showing that reduced TrxR1 expression level could directly increase BS resistance. The correlation between IC_{50} values (Table 3) and basal TrxR levels (Fig. S3A) of three HCC cell lines also revealed that BS is an inhibitor of TrxR1. Gan et al. also showed that TrxR antisense RNA suppress growth of another HCC cell line SMMC-7721 by inducing G2/M arrest, increasing p53 and decreasing Bcl-2 mRNA levels [41]. To our surprise, the NADPH oxidase inhibitor DPI, instead of mitochondrion inhibitor MT, significantly lessened ROS induced by BS (Fig. 6F), since the potential target of BS -TrxR2 is located in mitochondrion. It has been reported that the inhibition of TrxR C-terminal active site selenocysteine would induce strong NADPH oxidase activity of TrxR, promote its pro-oxidant effects and rapidly cause cell death [42]. Small molecules targeting TrxR have been proved to shift TrxR to NADPH oxidase to produce ROS, like parthenolide [43], curcumin [44] and juglone [45]. Therefore, we speculated that mitochondrial TrxR2 may also be shifted to act as NADPH oxidase. Although we have demonstrated that ROS was significantly increased after either BS treatment or TrxR1 downregulation in HCC cells, the exact influence of long-term (24 weeks) and low-dose (9–36 mg/kg) BS treatment on hepatic cells, fibroblast and other liver cells remains to be answered in further studies. As TrxR is a selenoprotein, we speculate that the selenium of BS may be metabolized to synthesize TrxR to scavenge ROS induced by DEN during hepatocarinogenesis [46].

BS treatment could induce G2/M arrest and apoptosis in HepG2 cells. Trx has been proved to interact with Ref-1 to activate AP-1 through nuclear translocation [47]. Ref-1 can function as a redox factor to reduce transcription factors, including AP-1 and NF-κB, and has been taken as a therapeutic and chemopreventive target [48]. In mammals, AP-1 regulates cell cycle through cyclin D and p21, influencing G1/S and G2/M phase progression [49]. In our study, both gene and protein level of Ref-1 were down-regulated by BS treatment (Fig. 7D and E), implying that AP-1 activation would also be suppressed by BS and lead to G2/M arrest in HepG2 cells (Fig. 5B). Besides, significant apoptosis was observed after 20–40 μM BS exposure for 24 h in HepG2 cells (Fig. 5C), which may explain the pronounced proliferative inhibition against HepG2, Bel7402 and Huh7 cells (Fig. 5A). Since NF-κB pathway is involved in apoptosis regulation [11], Bax, Bcl-2 and Caspase-3 expression were explored and results proved that BS induced mitochondria-dependent apoptosis in HepG2 cells. The G2/M arrest and apoptosis induction of BS may explain the significant tumor volume decrement and prolonged tumor formation in mice models implanted with 1×10^4–1×10^6 H22 cells (Fig. 4). Similar to our data, another HCC chemopreventive compound curcumin also triggers apoptosis, anti-inflammation and anti-proliferation by downregulating AP-1 and NF-κB pathways *etc.* [50].

In conclusion, the organoselenium-containing BS exerted preventive effect on hepatocellular injury-cirrhosis-HCC process in chemically induced mice models without significant immunosuppression. Besides, BS treatment could increase ROS level, induce G2/M arrest and apoptosis in HCC cells so that HCC formation could be significantly inhibited and tumors remarkably shrinked. The TrxR and NF-κB pathway downregulation may contribute to prevention of BS against hepatocarcinogenesis. More *in vivo* studies are necessary to confirm the preventive function of BS, especially at the stage from cirrhosis to HCC; *in vitro* experiments should also be practiced to explore the precise sources of ROS induced by BS and the effects of BS on hepatic cells, fibroblast cells and vascular cells. Based on the results, BS may be a chemopreventive strategy to reduce HCC incidence in the future, especially in selenium deficient areas.

Funding

This work was funded by the National Natural Science Foundation of China (81372266) and National Science and Technology Major Project, People's Republic of China (2011zx09101-001-03).

Conflict of interests

The authors declared that they had no conflict of interest.

Acknowledgements

We thank Dr. Siwang Yu for providing animal lab. We thank pathologist Fei Pei for examining liver tissues. We thank Bo Xu, Yongrui Jia, Shuqin Xin and Yufang Sun for their technical help.

Appendix A. Supplementary material

Supplementary data associated with this article can be found in the online version at http://dx.doi.org/10.1016/j.redox.2017.09.014.

References

[1] L.A. Torre, F. Bray, R.L. Siegel, J. Ferlay, J. Lortet-Tieulent, A. Jemal, Global cancer statistics, 2012, CA: Cancer J. Clin. 65 (2015) 87–108.
[2] H.B. El-Serag, K.L. Rudolph, Hepatocellular carcinoma: epidemiology and molecular carcinogenesis, Gastroenterology 132 (2007) 2557–2576.
[3] A. Forner, J.M. Llovet, J. Bruix, Hepatocellular carcinoma, Lancet (Lond. Engl.) 379 (2012) 1245–1255.
[4] C.R. de Lope, S. Tremosini, A. Forner, M. Reig, J. Bruix, Management of HCC, J. Hepatol. 56 (2012) S75–S87.
[5] K. Katanoda, T. Matsuda, Five-year relative survival rate of liver cancer in the USA, Europe and Japan, Jpn. J. Clin. Oncol. 44 (2014) 302–303.
[6] G. Ercolani, G.L. Grazi, M. Ravaioli, M. Del Gaudio, A. Gardini, M. Cescon, G. Varotti, F. Cetta, A. Cavallari, Liver resection for hepatocellular carcinoma on cirrhosis: univariate and multivariate analysis of risk factors for intrahepatic recurrence, Ann. Surg. 237 (2003) 536–543.
[7] T.W. Kensler, P.A. Egner, J.-B. Wang, Y.-R. Zhu, B.-C. Zhang, P.-X. Lu, J.-G. Chen, G.-S. Qian, S.-Y. Kuang, P.E. Jackson, S.J. Gange, L.P. Jacobson, A. Muñoz, J.D. Groopman, Chemoprevention of hepatocellular carcinoma in aflatoxin endemic areas, Gastroenterology 127 (2004) S310–S318.
[8] Y. Hoshida, B.C. Fuchs, N. Bardeesy, T.F. Baumert, R.T. Chung, Pathogenesis and prevention of hepatitis C virus-induced hepatocellular carcinoma, J. Hepatol. 61 (2014) S79–S90.
[9] S. Bruno, T. Stroffolini, M. Colombo, S. Bollani, L. Benvegnu, G. Mazzella, A. Ascione, T. Santantonio, F. Piccinino, P. Andreone, A. Mangia, G.B. Gaeta, M. Persico, S. Fagiuoli, P.L. Almasio, Sustained virological response to interferon-alpha is associated with improved outcome in HCV-related cirrhosis: a retrospective study, Hepatology 45 (2007) 579–587.
[10] P. Greenwald, Cancer chemoprevention, BMJ (Clin. Res. Ed.) 324 (2002) 714–718.
[11] E. Pikarsky, R.M. Porat, I. Stein, R. Abramovitch, S. Amit, S. Kasem, E. Gutkovich-Pyest, S. Urieli-Shoval, E. Galun, Y. Ben-Neriah, NF-kappaB functions as a tumour promoter in inflammation-associated cancer, Nature 431 (2004) 461–466.
[12] H.L. Pahl, Activators and target genes of Rel/NF-kappaB transcription factors, Oncogene 18 (1999) 6853–6866.
[13] J.M. Heilman, T.J. Burke, C.J. McClain, W.H. Watson, Transactivation of gene expression by NF-kappaB is dependent on thioredoxin reductase activity, Free Radic. Biol. Med. 51 (2011) 1533–1542.
[14] E.S. Arner, Focus on mammalian thioredoxin reductases–important selenoproteins with versatile functions, Biochim. Biophys. Acta 1790 (2009) 495–526.
[15] C. Li, Y. Peng, B. Mao, K. Qian, Thioredoxin reductase: a novel, independent prognostic marker in patients with hepatocellular carcinoma, Oncotarget 6 (2015) 17792–17804.
[16] E.S. Arner, A. Holmgren, The thioredoxin system in cancer, Semin. Cancer Biol. 16 (2006) 420–426.
[17] X. Zheng, W. Xu, R. Sun, H. Yin, C. Dong, H. Zeng, Synergism between thioredoxin reductase inhibitor ethaselen and sodium selenite in inhibiting proliferation and inducing death of human non-small cell lung cancer cells, Chem.-Biol. Interact. 275 (2017) 74–85.
[18] V. Vichai, K. Kirtikara, Sulforhodamine B colorimetric assay for cytotoxicity screening, Nat. Protoc. 1 (2006) 1112–1116.
[19] S.E. Eriksson, S. Prast-Nielsen, E. Flaberg, L. Szekely, E.S. Arner, High levels of thioredoxin reductase 1 modulate drug-specific cytotoxic efficacy, Free Radic. Biol. Med. 47 (2009) 1661–1671.
[20] Y. Zhang, X. Zhang, X. Wang, L. Gan, G. Yu, Y. Chen, K. Liu, P. Li, J. Pan, J. Wang, S. Qin, Inhibition of LDH-A by lentivirus-mediated small interfering RNA suppresses intestinal-type gastric cancer tumorigenicity through the downregulation of Oct4, Cancer Lett. 321 (2012) 45–54.
[21] X. Cheng, P. Holenya, S. Can, H. Alborzinia, R. Rubbiani, I. Ott, S. Wolfl, A. TrxR, inhibiting gold(I) NHC complex induces apoptosis through ASK1-p38-MAPK signaling in pancreatic cancer cells, Mol. Cancer 13 (2014) 221.
[22] I. Rahman, A. Kode, S.K. Biswas, Assay for quantitative determination of glutathione and glutathione disulfide levels using enzymatic recycling method, Nat. Protoc. 1 (2006) 3159–3165.

[23] A. Glasauer, N.S. Chandel, Targeting antioxidants for cancer therapy, Biochem. Pharmacol. 92 (2014) 90–101.
[24] P.W. Vesely, P.B. Staber, G. Hoefler, L. Kenner, Translational regulation mechanisms of AP-1 proteins, Mutat. Res. 682 (2009) 7–12.
[25] M. Luo, F. Yang, S.X. Huang, Z.P. Kuang, X.L. Luo, Y.D. Li, J.N. Wu, Y.A. Xie, Two-stage model of chemically induced hepatocellular carcinoma in mouse, Oncol. Res. 20 (2013) 517–528.
[26] F. Heindryckx, I. Colle, H. Van Vlierberghe, Experimental mouse models for hepatocellular carcinoma research, Int. J. Exp. Pathol. 90 (2009) 367–386.
[27] S.A. Sheweita, M.A. El-Gabar, M. Bastawy, Carbon tetrachloride changes the activity of cytochrome P450 system in the liver of male rats: role of antioxidants, Toxicology 169 (2001) 83–92.
[28] S. Bandiera, C. Billie Bian, Y. Hoshida, T.F. Baumert, M.B. Zeisel, Chronic hepatitis C virus infection and pathogenesis of hepatocellular carcinoma, Curr. Opin. Virol. 20 (2016) 99–105.
[29] M. Capurro, I.R. Wanless, M. Sherman, G. Deboer, W. Shi, E. Miyoshi, J. Filmus, Glypican-3: a novel serum and histochemical marker for hepatocellular carcinoma, Gastroenterology 125 (2003) 89–97.
[30] R.T. Poon, I.O. Ng, C. Lau, W.C. Yu, Z.F. Yang, S.T. Fan, J. Wong, Tumor microvessel density as a predictor of recurrence after resection of hepatocellular carcinoma: a prospective study, J. Clin. Oncol.: Off. J. Am. Soc. Clin. Oncol. 20 (2002) 1775–1785.
[31] W.M. Coston, S. Loera, S.K. Lau, S. Ishizawa, Z. Jiang, C.L. Wu, Y. Yen, L.M. Weiss, P.G. Chu, Distinction of hepatocellular carcinoma from benign hepatic mimickers using Glypican-3 and CD34 immunohistochemistry, Am. J. Surg. Pathol. 32 (2008) 433–444.
[32] S. Kumar, A. Holmgren, Induction of thioredoxin, thioredoxin reductase and glutaredoxin activity in mouse skin by TPA, a calcium ionophore and other tumor promoters, Carcinogenesis 20 (1999) 1761–1767.
[33] J. Yodoi, T. Tursz, ADF, a growth-promoting factor derived from adult T cell leukemia and homologous to thioredoxin: involvement in lymphocyte immortalization by HTLV-I and EBV, Adv. Cancer Res. 57 (1991) 381–411.
[34] J.H. Choi, T.N. Kim, S. Kim, S.H. Baek, J.H. Kim, S.R. Lee, J.R. Kim, Overexpression of mitochondrial thioredoxin reductase and peroxiredoxin III in hepatocellular carcinomas, Anticancer Res. 22 (2002) 3331–3335.
[35] L. Bjorkhem, H. Teclebrhan, E. Kesen, J.M. Olsson, L.C. Eriksson, M. Bjornstedt, Increased levels of cytosolic thioredoxin reductase activity and mRNA in rat liver nodules, J. Hepatol. 35 (2001) 259–264.
[36] J. He, D. Li, K. Xiong, Y. Ge, H. Jin, G. Zhang, M. Hong, Y. Tian, J. Yin, H. Zeng, Inhibition of thioredoxin reductase by a novel series of bis-1,2-benzisoselenazol-3(2H)-ones: organoselenium compounds for cancer therapy, Bioorg. Med. Chem. 20 (2012) 3816–3827.
[37] L. Zhang, Q. Cheng, Y. Wang, G.F. Merrill, T. Ilani, D. Fass, E.S. Arner, J. Zhang, Serum thioredoxin reductase is highly increased in mice with hepatocellular carcinoma and its activity is restrained by several mechanisms, Free Radic. Biol. Med. 99 (2016) 426–435.
[38] A.M. Elsharkawy, D.A. Mann, Nuclear factor-kappaB and the hepatic inflammation-fibrosis-cancer axis, Hepatology 46 (2007) 590–597.
[39] M.A. Rahman, D.K. Dhar, E. Yamaguchi, S. Maruyama, T. Sato, H. Hayashi, T. Ono, A. Yamanoi, H. Kohno, N. Nagasue, Coexpression of inducible nitric oxide synthase and COX-2 in hepatocellular carcinoma and surrounding liver: possible involvement of COX-2 in the angiogenesis of hepatitis C virus-positive cases, Clin. Cancer Res.: Off. J. Am. Assoc. Cancer Res. 7 (2001) 1325–1332.
[40] T. Wu, Cyclooxygenase-2 in hepatocellular carcinoma, Cancer Treat. Rev. 32 (2006) 28–44.
[41] L. Gan, X.L. Yang, Q. Liu, H.B. Xu, Inhibitory effects of thioredoxin reductase antisense RNA on the growth of human hepatocellular carcinoma cells, J. Cell. Biochem. 96 (2005) 653–664.
[42] Q. Cheng, W.E. Antholine, J.M. Myers, B. Kalyanaraman, E.S. Arner, C.R. Myers, The selenium-independent inherent pro-oxidant NADPH oxidase activity of mammalian thioredoxin reductase and its selenium-dependent direct peroxidase activities, J. Biol. Chem. 285 (2010) 21708–21723.
[43] D. Duan, J. Zhang, J. Yao, Y. Liu, J. Fang, Targeting thioredoxin reductase by parthenolide contributes to inducing apoptosis of HeLa cells, J. Biol. Chem. 291 (2016) 10021–10031.
[44] J. Fang, J. Lu, A. Holmgren, Thioredoxin reductase is irreversibly modified by curcumin: a novel molecular mechanism for its anticancer activity, J. Biol. Chem. 280 (2005) 25284–25290.
[45] N. Cenas, H. Nivinskas, Z. Anusevicius, J. Sarlauskas, F. Lederer, E.S. Arner, Interactions of quinones with thioredoxin reductase: a challenge to the antioxidant role of the mammalian selenoprotein, J. Biol. Chem. 279 (2004) 2583–2592.
[46] J. Lu, C. Jiang, Selenium and cancer chemoprevention: hypotheses integrating the actions of selenoproteins and selenium metabolites in epithelial and non-epithelial target cells, Antioxid. Redox Signal. 7 (2005) 1715–1727.
[47] S.J. Wei, A. Botero, K. Hirota, C.M. Bradbury, S. Markovina, A. Laszlo, D.R. Spitz, P.C. Goswami, J. Yodoi, D. Gius, Thioredoxin nuclear translocation and interaction with redox factor-1 activates the activator protein-1 transcription factor in response to ionizing radiation, Cancer Res. 60 (2000) 6688–6695.
[48] M.L. Fishel, M.R. Kelley, The DNA base excision repair protein Ape1/Ref-1 as a therapeutic and chemopreventive target, Mol. Asp. Med. 28 (2007) 375–395.
[49] E. Shaulian, M. Karin, AP−1 as a regulator of cell life and death, Nat. Cell Biol. 4 (2002) E131–E136.
[50] A. Duvoix, R. Blasius, S. Delhalle, M. Schnekenburger, F. Morceau, E. Henry, M. Dicato, M. Diederich, Chemopreventive and therapeutic effects of curcumin, Cancer Lett. 223 (2005) 181–190.